IMPROVEMENT OF SODIUM FAST REACTOR CONTROL RODS CALCULATIONS WITH APOLLO3®

H. Guo, G. Martin, L. Buiron

Alternative Energies and Atomic Energy Commission
CEA, DEN, SPRC, F-13108 Saint-Paul Les Durance Cedex
Email: hui.guo@cea.fr

ABSTRACT

CEA is largely involved in the study of GEN-IV Sodium Fast Reactors (SFR). Some innovative reactivity control systems are proposed such as utilization of different absorbers or moderators materials, modification of absorber pin geometry, and application of burnable neutron poison. These designs possess potentials to improve its safety margin, economical performance or core characteristics while its complete analysis requires notably more accurate calculation of efficiency and evolution of isotopes' concentrations under irradiation.

At the same time, the new determinist transport code APOLLO3® is under development at CEA and it will replace ERANOS code for fast reactors analysis. The scheme in APOLLO3® is constituted with two steps: sub-assembly calculation and core calculation with Multi-Parametric Output Library as connectors which enable the interpolation of cross-sections according to specific parameter. In this paper, each step and different cross-section scheme are detailed and validated by continuous energy Monte Carlo calculations. These results are also compared with determinist code system ERANOS.

Our works show high adaptability of TDT solver in APOLLO3® to complexes geometries and evolution of isotopes. With the ability of MINARET to treat unstructured mesh, the heterogeneous geometry, keeping absorber pins at core level calculation, improves significantly the calculation of control rods' efficiency. APOLLO3® compute more accurately core's reactivity variation with burn-up tabulated cross section scheme. Although variation of spatial self-shielding effect is very significant in absorber depletion, tabulated cross-sections scheme is able to bring this variation from sub-assembly calculation to core calculation. Hence, even homogeneous control rod description at core level shows accurate computation of reactivity variation.

Consequently, with development and validations, APOLLO3® *shows improvement on SFR control rods neutronic simulation and analysis. With these new schemes presented in this paper, innovative reactivity control systems designs will be completely characterized and investigated in the near future.*

I. INTRODUCTION

Current control rods sub-assemblies in Fast Reactors (FR) adopt generally B4C as absorber material because of its high absorption ability from ^{10}B. However, B_4C generates gas, heat and pellet swelling during irradiation of neutrons. These effects reduce its residence time and safety margin. CEA is largely involved in the study of a GEN-IV Sodium Fast Reactor (SFR) especially in the prototype project – ASTRID[1]. This would be an opportunity to explore innovative reactivity control systems for fast reactors.

Self-breeder cores in current designs reduce the excess reactivity at beginning of cycle and hence the need of large controls rods margin. This advantage allows the use of reduced efficiency absorber materials such as europium, gadolinium, hafnium, and so on. However, accurate simulation of their depletion under irradiation would be required because the reactivity worth variation of low ^{10}B enriched B_4C would be not negligible, while materials such as hafnium and gadolinium process complex depletions chains and absorption resonance. Beside alternative absorber materials to B_4C, improved absorber pin size and application of moderator materials would also be potential candidates to innovative designs. And their evaluation requires the ability to treat complex geometry in details.

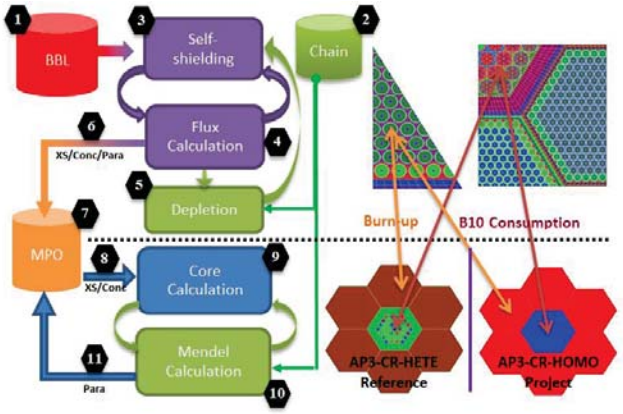
At same time, a determinist transport code called APOLLO3® is under development at CEA. It will replace ERANOS code for fast reactors analysis. Unstructured adaptive mesh S_N solvers (MINARET)[2], as well as 2-D and 3-D Method of Characteristic's (MOC) are already implemented in APOLLO3®[3]. This recent neutronic transport code would be suitable for the evaluation of control rods sub-assemblies in GIV fast reactors and some challenge design works. This paper focus on the development and validation of calculation schemes in APOLLO3® for SFR especially for the simulation of control rods. These schemes developed in APOLLO3® use rich feedback from determinist code ERANOS[4] and are validated by Monte-Carlo method TRIPOLI-4®[5].

SFR-3600-MOX is one of the SFR reactors concepts of the Generation-IV nuclear energy studied in an

international collaboration benchmark conducted by the Working Party on Scientific issues of Reactor Systems (WPRS) of the OECD/NEA[6]. Eleven international organizations contributed to this benchmark with different neutronic data library and transport code. This benchmark includes calculations of several key parameters of core and offers rich feedback of neutronic simulation. Therefore, this benchmark is a good reference for validation of newly developed schemes in APOLLO3®. The detailed description of WPRS/SFR-3600-MOX can be found in the Reference [6].

II. SCHEME DESCRIPTIONS

The calculation scheme for SFR using APOLLO3® contains two calculation steps as shown in Fig 1: sub-assembly calculation followed by core calculation. We present as follow the details of these two and they are compared with ERANOS and validated by TRIPOLI-4® in this paper.



XS: Cross-sections; Conc: Concentration; Para: Parameter; AP3-CR-HETE: Heterogeneous controls rods in geometries of core calculation; AP3-CR-HOMO: Homogeneous control rods in geometries of core calculation

Fig 1. APOLLO3® depletion calculation schemes

II.A. Description of cross-section and chains libraries

The JEFF-3.1.1 nuclear data library used in this paper is processed with the GALILEE[7] system to produce multi-group cross-sections set and probability tables of resonant isotopes in a 1968 groups structure. The elastic, inelastic and (*n, xn*) transfer matrices are distinguished with description up to P5 Legendre order expansion. The Legendre order expansion is limited as P1 in this paper. The influence of Legendre order expansion is already discussed in Reference [8].

The chain, especially the description of fission products, has important influence on the variation of reactivity in depletion calculations. In this paper, the depletion chain data for APOLLO3® uses explicit fission products with relevant data from evaluated files or tuned data from experiments. This depletion chain contains 126 fission products, 26 actinides and 5 additional isotopes. In comparison with a reference chain with far more isotopes (885 fission products and 26 actinides), it gathers the 99.9% of the reactivity loss in a SFR[9]. The sub-assembly calculation and core calculation shares the same chains data.

II.B. Description of sub-assembly calculation

Sub-assembly calculations aim to produce a homogenized (from exact geometries to simplified geometries) and collapsed (from 1968 to 33 groups) cross-sections library for the core calculation.

Sub-assembly calculations adopt the exact geometries of the fuel, fertile, control rods and other structures. Fig 2 shows different geometries of SFR-3600 MOX that are treated in sub-assembly calculation. The fuel sub-assemblies are described alone with reflective conditions. And for other structures sub-assemblies calculation, clusters contain both structure zones and fuel zones where the fuel zone has the objective to produce a representative neutrons spectrum. Except for the new Reflectors-Fuel cluster calculations, all sub-critical cluster calculation is set also with reflective conditions. Although B1 homogeneous leakage model and B heterogeneous leakage model are already available and validated in APOLLO3®[10], no leakage model is used in this paper and it would be studied in the near-future.

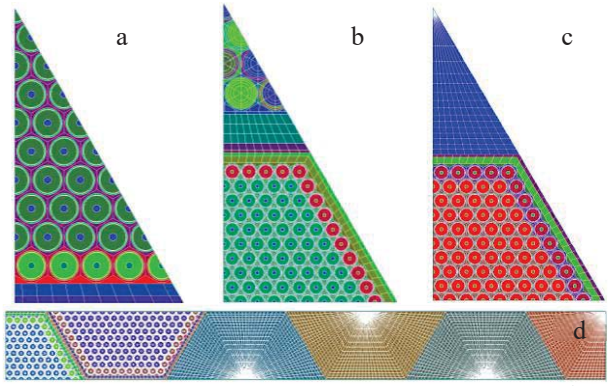


Fig 2. Geometries of S/A in SFR-3600 MOX a) 1/12th of Fuel sub-assembly. b) 1/12th CSD-Fuel cluster. c) 1/12th CSD Follower-Fuel cluster. d) Reflectors-Fuel cluster.

As shown in Fig 2, there are four reflector S/As with void boundary condition on its right side and reflective on other sides. The key for sub-assembly calculation is to use representative spectrum and distribution of flux for the self-shielding, homogenization and collapsing computations. To simulate the slowing-down effect of neutrons from the fuel zone to the reflector, a large cluster

with multi fuel and reflectors S/As is proposed[11], and it's also adapted in our works. As shown in Fig 2 (b), the Reflector-Fuel cluster contains two fuel S/As and four reflector S/As. Each reflector S/A in this cluster is homogenized to one independent cross-section set which will be associated with its correspondent reflector S/A in the core calculation.

The sub-assembly calculation contains two steps: self-shielding calculation and flux calculation. The sub-assembly calculation in this paper is achieved by Two/Three Dimensional Transport (TDT) solvers in APOLLO3®. The self-shielding calculation is calculated with *Pij* method using TDT-CPM solver with probability tables available in the 1968 groups' library. Then the flux calculation is done with MOC solver (TDT-MOC). TDT is able to treat not only two dimensions but also three dimensions geometries[3][12]. In this paper only 2-D MOC in APOLLO3® is used. 3D-MOC is a excepted method to compute axial heterogeneous configuration such as the fuel S/A in ASTRID-CFV[12], and the control rods when they parked at critical position. To ensure the angular and spatial convergence of flux, some improved tracking parameters for TDT is used in this work[8].

After convergence of self-shielding calculation and flux calculation, the fine cross-sections is collapsed into a broader energy group (33 groups in this works) and homogenized into larger regions according to the needs in the core calculation. The homogenization techniques used in this work is the classical flux-volume approach. More homogenization techniques combined with/without leakage models are already available in APOLLO3® and their validation with this benchmark would be a part of future works. At the end of sub-assemblies calculation, these cross-sections are stored in the Multi-Parametric Output library (MPO) files, which will be used later in core calculation. MPO contains tabulated cross-sections according to some parameters such as time value, burn-up, temperature and concentration of isotopes. If other core states are required such as sodium voiding case or change in material temperature, the material would be settled at these wanted states to calculate their cross-sections and store its indicated parameter. The neutronic data, mainly the reaction rate at normal state and depletion chain data, are passed to the MENDEL depletion solver. MENDEL[13] aims of succeeding current depletion solver DARWIN[14] and is a depletion solver for both Monte Carlo TRIPOLI-4® and deterministic APOLLO3® transport code systems. The result of depletion, i.e. the depleted isotopes concentrations, is then returned to execute next time step calculation.

II.C. Description of core calculation

As shown in Fig 1, after homogenization process in sub-assembly calculation, except for the control rods, the sub-assemblies in the core configuration are considered as hexagonal. In our study, two core geometry schemes distinguished by the geometry of control rods in core calculation are considered:

1) Homogeneous controls rods configuration (shortened in AP3-CR-HOMO) takes control rods S/A as a homogenous hexagon.

2) Heterogeneous controls rods configuration (shortened in AP3-CR-HETE) keeps the absorber pins in the hexagon of controls rods.

Each region in core geometry referred to the isotopes concentration and the cross-section in associated MPO file. For the active zone, the concentration and cross-section come from the homogenization of a Fuel subassembly i.e. Fig 2.a. For other regions, the concentration and cross-section come solely from the homogenization of the structure zones in the clusters with fuel sub-assembly. This homogenization can be complete or partial according to its corresponding geometries in the core. For instance, the control rod sub-assembly in Fig 2.b can be homogenized into one single region for AP3-CR-HOMO scheme. However, AP3-CR-HETE scheme homogenize each absorber pin control rods as independent region and the remains structures as one other region.

The AP3-CR-HETE core geometry for SFR-3600 MOX is shown in Fig 3. We then used the transport S_N solver MINARET[2] for the core calculation. this solver offer also a new flexibility in the symmetry of core geometry because of its ability to treat both structured and unstructured geometries. As shown in Fig 3, the SFR-3600 MOX is reduced to one sixth of its original core with reflective boundary condition at the top side and the lower right side. This symmetry option accelerates significantly the calculation.

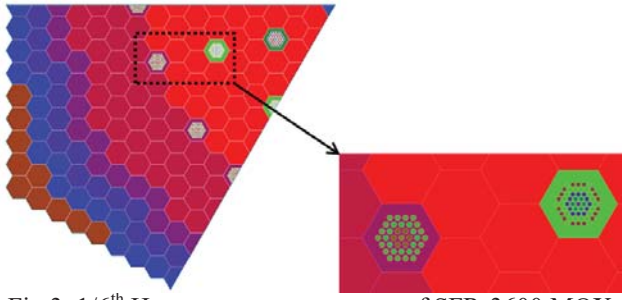


Fig 3. 1/6th Heterogeneous geometry of SFR-3600 MOX

To reach angular and spatial convergence, we use S6 level-symmetric quadrature (72 directions) with DGLP11 finite element type. The mesh size is 5 cm for the axial discretization and 36 triangles by hexagon (radial discretization) which leads to about 345 100 cells for AP3-CR-HOMO core configuration and 2 348 920 cells for the AP3-CR-HETE core configuration. MINARET also contains several features to speed up the resolution of the transport equation: MPI parallel computation

(parallelism on angular directions), DSA method and Chebyshev acceleration[8].

The flux calculation is performed using MINARET[2] solver in this works. The use of other solver: PASTIS or MINOS[15] will be studied in the future. Then core physic data are passed to MENDEL depletion solver which returns isotopes concentration for next step calculation. Three cross-section schemes are tested:

1) Constant XS: the calculation uses the updated concentrations from MENDEL solver while the isotopic cross-sections remain constant;

2) Variable XS: the calculation uses the updated concentrations from MENDEL solver and interpolates the cross-sections from MPO according to its time parameter.

3) Macro XS: the calculation interpolates both cross-sections and concentration from MPO according to its time parameter.

If calculations of other core states are needed in certain time step, the cross-sections are loaded from its relative MPO files with one of previous cross-sections scheme. According to the benchmark, there are four core states expected to be estimated: normal, sodium void, Doppler and control rods inserted.

III. SUB-ASSEMBLY VALIDATION

III.A. Fuel sub-assembly calculation

In this section, we focus in a simple depletion case that is SFR-3600 MOX fuel sub-assembly, as shown in Fig 2.a, with reflective boundaries. This case will help us to validate the depletion calculation of TDT, to study the influence of cross-sections schemes in core calculation and would contribute to the future uncertainty analysis[16].

In this simple case, APOLLO3® sub-assembly calculation considers the detailed geometry and core calculation uses homogenized hexagonal tube with reloading of cross-sections from sub-assembly calculation. The three previous cross-section schemes are applied in the core calculation and burn-up of fuel is chosen as time parameter for Variable XS and Macro XS scheme. The evolution of its reactivity, void worth and Doppler constant are calculated in this work with two determinist transport codes: APOLLO3® and ERANOS, and one Monte-Carlo transport code, TRIPOLI-4® as reference.

The ERANOS calculation scheme is close to APOLLO3® calculation with constant XS scheme in the core level calculation while it uses ECCO[17] to generate the self-shield cross-sections at beginning of evolution and VARIANT solver[18] for the core evolution calculation. ERANOS uses two different chains: one is pseudo-fission products chain and the other one is explicit chain while both of them are different from the chain used in APOLLO3®. The TRIPOLI-4® uses detailed geometry and continuous data and continuous energy nuclear data library. TRIPOLI-4® and APOLLO3® share the same explicit depletion chains and depletion solver in this works. The purpose of this sub-assembly depletion benchmark is to investigate the different calculation schemes and hence all of them share same data library JEFF3.1.1. The influence of data library was studied in detail in Reference [16].

The variation of reactivity with time of this simple case is shown in Table I. The power generated is normalized to 50 W per gram of heavy nucleus (HN) and the irradiation time is 410 Equivalent Full Power Day (EFPD) dividing into four equal time steps. Firstly, different codes show high coherence in the BOEC reactivity calculation. The result from TDT solver in APOLLO3® has only several pcm discrepancy from TRIPOLI-4® calculation if multi-groups fission spectrum is used. With one average fission group, TDT solver, MINARET and ERANOS underestimates the reactivity about 50 pcm by comparing with Monte-Carlo reference. However, the fission spectrum has very slight influence on the reactivity variation according to TDT solver's results.

Table I : Variation of Reactivity with time in infinite fuel sub-assembly from different codes

Time (EFPD)	0	410	Variation
TRIPOLI-4®[16]	11756	12189	433
ERANOS			
Explicit Chain[16]	11708	12325	617
ps-FP Chain	11708	12112	404
APOLLO3-TDT			
4 Fission Groups	11760	12165	404
1 Fission Group	11704	12113	410
APOLLO3-MINARET			
Constant XS	11703	12164	461
Variable XS	11703	12110	407
Macro XS	11703	12106	403

At EOEC, the TRIPOLI-4® shows an increase of reactivity about 433 pcm while TDT solver under-estimate this increase about 30 pcm. The fuel S/A's reactivity increases with time (during one cycle i.e. 410 EFPD) because SFR-3600 MOX is self-breeder design without specific blanket zones. TDT solver generates self-shielded cross-section for core calculation. The reactivity variation from MINARET solver is very close to one obtained with TDT solver if Variable XS scheme or Macro XS scheme is used. However, MINARET Constant XS Scheme over-estimates the increase of reactivity about 60 pcm by comparing with Variable XS scheme. The explicit chain in ERANOS over-estimates the variation of reactivity about 184 pcm by comparing with TRIPOLI-4® result while ps-FP chains underestimate

about 30 pcm. The variation of reactivity in ERANOS with ps-FP model is close to TDT while ERANOS use Constant XS scheme. If the influence of cross-sections' variation is considered, the ps-FP calculation underestimates about 90 pcm reactivity increase by comparing with TRIPOLI-4® while its explicit chain calculation overestimates about 124 pcm. Although ps-PF model shows a better "accuracy" in the reactivity calculation, associated uncertainty study needs the concentration of real fission production and hence an explicit chain. The more detailed benchmarks with same depletions chains and different neutronic library will be continued between ERANOS and APOLLO3®.

The sodium void worth and Doppler Constant are two important "safety" parameters for the core physic study. They are calculated for both fuel sub-assembly depletion benchmark and core depletion benchmark. In this benchmark, the sodium void worth is defined by the reactivity change between the sodium voided and normal states such as:

$$\Delta\rho = \rho_{void} - \rho_{normal}$$

where the subscripts void and normal indicate the sodium voided and normal states, respectively. In this benchmark, the sodium voided state is defined by voiding all sodium in the active core, which contains the inner and outer fuel zones in SFR-3600 MOX core.

The Doppler constant is defined by:

$$K_D = (\rho_{high} - \rho_{normal})/\ln(T_{high} - T_{normal})$$

where the subscript high indicates the perturbed core state. In this work, the high fuel temperature is a factor of two of that of the normal fuel temperature that means 3000 K in MOX materials.

The results from different code and different calculation schemes are shown in Table II and Table III. For the sodium void worth, if we take Monte-Carlo method as reference, APOLLO3®, both with TDT and MINARET solver, improve this parameter's accuracy about 60 ~ 70 pcm compared to ERANOS. And this parameter increases 89 pcm after 410 EFPD in TRIPOLI-4® calculation. APOLLO3-TDT solver computes almost same variation as Monte-Carlo method and is able to model the influence of depletion to MINARET solver if the variation of cross-section is considered in the core level calculation. Both ERANOS and Constant XS scheme in APOLLO3® under-estimate this increase of sodium void worth. For Doppler Constant, all solvers show coherence at BOEC with slight difference. With the variation of self-shielded cross-sections, Variable XS and Macro XS estimate the variation of this Doppler Effect in a better way than Constant XS scheme. The influence of different nuclear data library and their uncertainty would be also an interesting research direction with this simple model.

Table II. Benchmark of Sodium Void Worth in infinite fuel sub-assembly (unit: pcm)

Time (EFPD)	0	410	Variation
TRIPOLI-4®[16]	3090	3179	89
ERANOS[16]	2990	3031	41
APOLLO3-TDT	3057	3145	87
APOLLO3-MINARET			
Constant XS	3049	3106	57
Variable XS	3049	3134	85
Macro XS	3049	3133	84

Table III. Benchmark of Doppler Constant in infinite fuel sub-assembly (unit: pcm)

Time (EFPD)	0	410	Variation
TRIPOLI-4®[16]	-921	-802	120
ERANOS[16]	-918	-847	71
APOLLO3-TDT	-920	-809	111
APOLLO3-MINARET			
Constant XS	-920	-830	90
Variable XS	-920	-812	107
Macro XS	-920	-811	108

III.B. Control rods sub-assembly validation

Hereafter, we present the main results obtained with our calculation scheme for control rods cluster. The geometry for APOLLO3-TDT is shown in Fig 2.b where each control rods sub-assembly contains 37 absorber pins with natural B_4C. The geometries used in APOLLO3-MINARET are shown in Fig 4.a and Fig 4.b where CR-HOMO homogenize whole sub-assembly as hexagonal tube and CR-HETE keeps absorber pins' geometries in the core level calculation. Those results are compared with the continuous energy Monte Carlo TRIPOLI-4® code whose geometry is shown in Fig 4.c where each absorber pin is divided into 18 independent depletion zones to compute the heterogeneous distribution of reaction in these regions.

Both fuel and absorber are depleted and the power density is normalized as 50 W/g(HN). There are 4 equal length time steps between 0 and 410 EFPD.

The variation of reactivity of this cluster is shown in TABLE IV. The variation of reactivity is similar between APOLLO3-TDT and TRIPOLI-4®. APOLLO3-MINARET solver overestimates this variation while the Variable XS scheme improves this accuracy especially for CR-HOMO geometry.

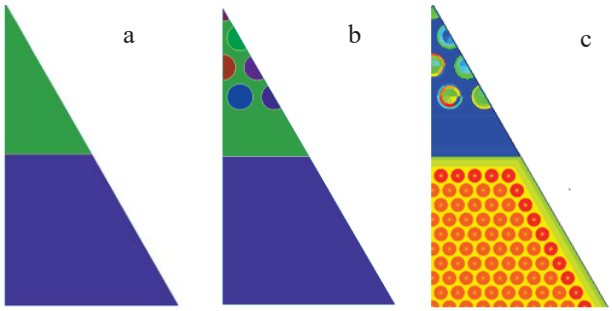


Fig 4. a) 1/12th of homogenous CSD-Fuel cluster used in MINARET (CR-HOMO). b) 1/12th of heterogeneous CSD-Fuel cluster used in MINARET (CR-HETE). c) 1/12th of CSD-Fuel cluster used in TRIPOPLI-4.

TABLE IV. Reactivity Variation of CSD-Fuel Cluster

Time (EFPD)		0	410	Variation
TRIPOLI-4®		-21189	-20101	1087
AP3-TDT		-21150	-20058	1092
APOLLO3-MINARET				
HOMO	Constant	-22530	-20885	1645
HETE	Constant	-21152	-19979	1173
HOMO	Variable	-22530	-21304	1226
HETE	Variable	-21152	-20066	1086

The ^{10}B absorption cross-sections used in the homogenous core level calculation is shown in Fig 5 where the absorber is homogenized into whole S/A. The flux gradient is large in absorber S/A. Furthermore, before arriving in the inner regions of absorber, neutrons in lower energy are already absorbed by the outer regions. This important gradient in the distribution of absorption reaction rate is so-called spatial self-shielding effect. For CR-HOMO calculation, the absorber is homogenized to whole S/A and hence this effect is accounted in the sub-assembly calculation level which leads to a reduced effective in the low energy domain (typically 1 keV). During irradiation, the outer region of absorber is depleted firstly which enable more neutrons travel to the inner region. And hence, the absorption reactions decrease in the outer region but increase in the inner region with consumption of absorber materials. Consequently, the spatial self-shielding effect is reduced with time and hence the effective absorption cross-section increase with time. Constant XS scheme does not compute the variation of screening effect with depletion and hence underestimate the absorption ability of absorber material. Variable XS scheme reload the XS according to its depletion and hence increase the calculation accuracy about 40 % with still 12.8 % overestimation.

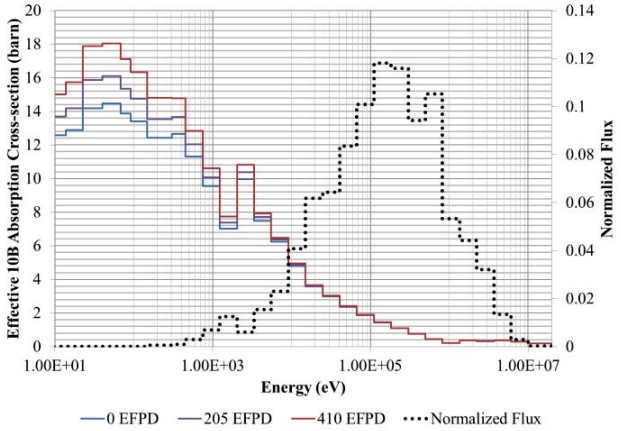


Fig 5. Variation of ^{10}B effective absorption cross-section with time and normalized flux at initial state (in 33 groups)

The cross-section homogenized for APOLLO3® heterogeneous geometry is close to its intuitive values because there is no homogenization for B_4C material (with flux-volume homogenization method) and the self-shielding effect raised from absorption resonance for B10 is negligible. However, if other materials such as hafnium and gadolinium are used as absorber material, the self-shielding effect should be considered with care in the S/A level calculation as they have important absorption resonances. As the keep of absorber pins in the core geometry, the spatial screening effect is well treated in core calculation. The difference of CR-HETE in TABLE IV comes from the XS scheme in the fuel part. The best-estimation from APOLLO3-MINARET has only 1 pcm difference from TRIPOLI-4®.

IV. CORE VALIDATION

IV.A. Core reactivity

Based on previous calculation in 2-D sub-assembly/cluster calculation, the benchmark of the SFR-3600-MOX is achieved to investigate the application of these schemes in the 3-D core. For calculation in this section, the thermal power is settled 3600 MW and the total depletion time is 410 EFPD which is divided into four steps with same length of time. In this part, only the fuel parts are depleted while other structures are considered as static materials. For the APOLLO3® calculations, three cross-section schemes are used for fuel zones with its burn-up as parameter to interpolate the cross-sections.

The reactivity of SFR-3600 MOX core is shown in TABLE V where APOLLO3®, TRIPOLI-4® and ERANOS use JEFF-3.1.1 cross-section data library. The APOLLO3® use homogenous geometry in core level calculation. The heterogeneous control rods geometry increases several pcm of core reactivity at BOEC and has almost no influence on the variation of core's reactivity because the anti-reactivity of control rods is not important

when they park outside the fissile zones. ERANOS results underestimate core reactivity by about 340 pcm while APOLLO3® overestimate by about 130 pcm comparing to Monte-Carlo results at BOEC. APOLLO3® shows improved core reactivity calculation compared to ERANOS and the overestimation of reactivity in APOLLO3® can be further reduced by other homogenization methods together with advanced leakage models[11] [19].

TABLE V. SFR-3600 MOX Core Reactivity (unit: pcm)

Code	XS Scheme	BOEC	EOEC	Variation
TRIPOLI-4®[6]	--	1931	1671	-260
ERANOS[6]	--	1594	1341	-252
APOLLO3®	Constant	2062	1857	-205
	Variable	2062	1796	-266
	Macro	2062	1997	-65

The reactivity variations from ERANOS and APOLLO3® Variable XS are close to TRIPOLI-4® result which is about -260 pcm. The influence of time mesh is also studied with APOLLO3® where reduced time mesh (one step for 410 EFPD) enlarge the reactivity loss about 9 pcm and fine time mesh (10 steps) reduce the reactivity loss about 1 pcm.

The Macro XS in APOLLO3® showed good performance in previous fuel sub-assembly calculation while it lost totally the accuracy in the core calculation. In the Macro XS scheme, not only the cross-section but also the isotopes concentrations are passed into the core calculation with burn-up in fuel as connection parameter. However, the flux spectrum and distribution in the core are always slightly different from its reference sub-assembly calculation because of the influence of other fuel zones and structures zones. And hence, at same burn-up, the concentration from core calculation is not the same as the one from sub-assembly calculation. Consequently, Macro XS scheme does not fit the whole core depletion.

The same as previous sub-assembly depletion benchmark, the Variable XS scheme shows better coherence with Monte-Carlo method for APOLLO3®. Constant XS scheme underestimates always about 60 pcm of reactivity loss by comparing with Variable XS scheme. The core calculation shows same phenomenon in the fuel depletion benchmark. The TRIPOLI-4® and APOLLO3® share complete chains and depletion solver, while ERANOS use ps-FP chain in core calculation. The reactivity variation from ERANOS has only several pcm differences from TRIPOLI-4® although it use Constant XS scheme. ERANOS ps-FP model shows a good reactivity variation, but a calculation with explicit chain is expected for the uncertainty study.

The Sodium Void Worth and Doppler Effect at BOEC and EOEC are summarized in TABLE VI where APOLLO3® use Variable XS scheme

In this benchmark, by comparing with ERANOS®, APOLLO3® does not improve the accuracy of void effect and Doppler Effect calculations. The more detailed study is needed for their improvement.

At EOEC three states: sodium void, Doppler Effect and control rods inserted are considered. For the Constant XS scheme, the sodium void worth, Doppler Effect constant at EOEC and their variation from BOEC of SFR 3600 MOX core is shown in TABLE VI. The structure and the multi-influence between fuel and structure are not well computed.

TABLE VI. SFR-3600 MOX Sodium Void Worth and DOPPLER Constant (unit: pcm)

Code	TRIPOLI-4®[6]	ERANOS[6]	APOLLO3®
Sodium Void Worth			
BOEC	1963	1931	2005
EOEC	2321	2056	2145
Variation	358	125	140
Doppler Constant			
BOEC	-982	-971	-992
EOEC	-834	-887	-896
Variation	148	84	96

The isotopes' concentration and flux distribution evaluate with time and hence these parameters. After one cycle irradiation, the sodium void worth from APOLLO3® is close to TRIPOLI-4® results with 176 pcm lower estimation using Variable XS scheme and with 205 pcm lower estimation using Constant XS scheme. TRIPOLI-4® shows a 358 pcm increase while the best estimation of determinist code comes from APOLLO3® Variable XS scheme but only with 140 pcm increase. The Doppler Effect decreases with time. ERANOS shows better absolute value and APOLLO3® Variable XS shows better variation.

IV.B. Control Rods Efficiency

Control rods S/A is the most important subcritical structure in the core. Stochastic codes are able to keep the "exact" geometries of control rod and use continuous energy. The deterministic approaches compute self-shielding effect in the sub-assembly calculation step and use homogenized geometries in the core level calculation. According to the benchmarks results[6], most deterministic approaches overestimate the control rod reactivity worth by comparing with stochastic approach.

The result from ERANOS® was performed with rod heterogeneity correction using an equivalence method [2].

In this method, the heterogeneous controls rods S/A is surrounded by homogenous fuel in a 2-D-XY model. This geometry is then solved by BISTRO 2-D S_N transport code[4] to get its direct and adjoint neutrons flux. Using the perturbation tool in the ERANOS®, the equivalent homogenized cross-section is corrected by the adjoint flux from its correspondent homogeneous model until the convergence of homogenous model's reactivity to the heterogeneous model's reactivity. The corrected cross-sections produced from this method are similar to the cross-section used in APOLLO3®, as shown in Fig 5 and will be used in the core level calculation. This method is developed to adapt depletion calculation and axial effects by D. Blanchet and M. Andersson[18] [19].

APOLLO3® does use exact geometries for fuel and structures in sub-assembly calculation which compute well the space effect and also the impact of absorber on the fuel. The homogenization technologies used here is flux-volume although moment homogenization technologies combined with/without leakage model are already validated for fuel part[10]. It would be interesting to study the influence of homogenization technologies and leakage effects. In the core level there are two different geometries: the homogenous core and heterogeneous core which is benefit from the ability of MINARET in the treatment of unstructured mesh.

I.A.1. Static calculation

In this section, we focused on WPRS/SFR-3600-MOX benchmark where control rods are not supposed to evolve under irradiation. The reactivity worth of control rods shown in TABLE VII is the difference of core's reactivity between all control rods park on the bottom and on the top of fissile region.

TABLE VII. SFR-3600 MOX Control Rods' Worth (units: pcm)

Code		BOEC	EOEC	Variation
TRIPOLI-4®[6]		-5624	-5792	-168
ERANOS[6]		-6217	-6364	-147
APOLLO3®				
HOMO	Constant	-6032	-6328	-296
HETE	Constant	-5797	-6066	-269
HOMO	Variable	-6032	-6301	-269
HETE	Variable	-5797	-6033	-236

For the APOLLO3® core calculation, 19 CPU of office computer use about 6 hours for one time step calculation of homogenous configuration and the heterogeneous configuration use about 5~6 times as that of homogenous configuration. Both APOLLO3® and ERANOS overestimate the efficiency of control rods at BOEC in this benchmark. However, by comparing with ERANOS, AP3-CR-HOMO geometry improves 185 pcm and AP3-CR-HETE geometry improves accuracy about 420 pcm. The best estimation of APOLLO3® has only about 173 pcm overestimation on control rods' efficiency. Furthermore, the reference of TRIPOLI-4® used here is in the previous benchmark. In our own calculation of TRIPOLI-4®, the difference between APOLLO3® and Monte-Carlo is only about 34 pcm.

With core flux distribution concentrate to the center core, the control rods efficiency increases slightly with time. This increase in APOLLO3® is more important than TRIPOLI-4® and ERANOS. However, all APOLLO3® results show an improved performance at the EOEC control rods efficiency calculation by comparing with ERANOS especially when APOLLO3® uses CR-HETE core configuration and Variable XS scheme. The best APOLLO3® results at EOEC over-estimate about 241 pcm by comparing with TRIPOLI-4®.

I.A.2. Depletion calculation

The more regular position for the control rods in the core is to keep the critical state of the core. The control rods insert into the fissile zone and the absorber material deplete with irradiation of neutrons.

Firstly, SFR-3600-MOX's control rods located at inner/outer interface are inserted 10 into the core. The anti-reactivity introduced by this insertion in TRIPOLI-4®, AP3-CR-HOMO and AP3-CR-HETE are respectively -127 pcm, -134 pcm and -133 pcm. The neutron spectrum and ^{10}B absorption in the insertion zone are compared between APOLLO3® and TRIPOLI-4®. The neutron spectrum in absorber material from AP3-CR-HETE calculation is consistent with results from TRIPOLI-4®. The AP3-CR-HOMO's result is slightly different from TRIPOLI-4® but its corrective cross-section reduces this difference in the absorption rate. The neutron spectrum obtained in cluster sub- calculation is "harder" than the one from core calculation because it's relatively compact geometry and lack of effects from other structures.

The relative ^{10}B absorption rate in Fig 6 is the ratio between the average reaction rate in absorber classified by its row and the average value in whole S/A. The spatial distribution increases from the center row to the external row. The difference between AP3-CR-HETE and TRIPOLI-4® is smaller than 0.8 % if the center pin (1/37 of whole absorber pins) is not considered where AP3-CR-HETE overestimation is roughly around 3.3%. Combined with previous sub-assembly calculation, this distribution validation ensures the correct evolution of CR-HETE in a 3-D core calculation.

The difference between APOLLO3® cluster calculation and the core calculation is less than 10 %. The gradient in cluster calculation is more important because there is less fuel to provide a flat flux. A larger control

rods cluster with more fuel region in subassembly calculation may improve its representativeness from the point of view that more similar flux spectrum and distribution in the sub-assembly calculation by comparing the core calculation would better simulate the self-shielding and spatial screening effects. Furthermore, when the control rods are parked at critical position, the neutrons arrived from its bottom is not negligible while the representative cluster is only a 2-D geometry which considers only the radial neutron distribution. The 3-D sub-assembly calculation or leakage model may helpful and the detailed development and validation needed to be done.

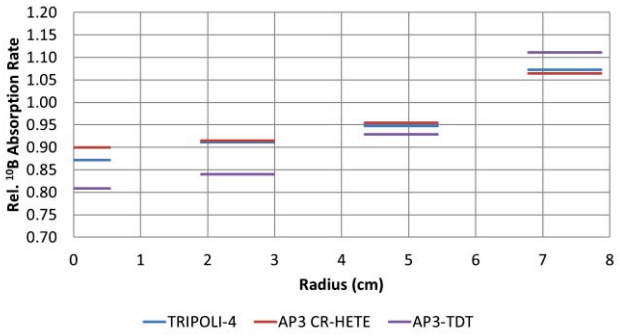


Fig 6. ^{10}B absorption spatial distribution (ring by ring) in the inserted parts of CSD (between C1 and C2, 10 cm inserted) and in CSD cluster

The efficiency in TABLE VIII is calculated for rods at inner core/outer core interface with 25 cm insertion when the 1/5th of fuel is reloaded every cycle ("real" equilibrium core with reloading pattern). Each cycle has 410 EFPD.

TABLE VIII. Evolution of control rods efficiency at critical position (units: pcm)

Geometry	HOMO	HOMO	HETE
Absorber	Static	Depleted	Depleted
1st BOEC	509	509	510
2nd BOEC	504	491	493
3rd BOEC	514	483	484
4th BOEC	515	463	464
5th BOEC	518	445	447
6th BOEC	526	430	432
Variation	17	-79	-78

If the absorber is not depleted, it's efficiency increase slightly because the flux spatial redistribution. The variation raised by the evolution of absorbers' isotopes is about 20 % of its initial efficiency according to AP3-CR-HETE Variable XS scheme. And then the depletion of control rods is also compared between CR-HETE and CR-HOMO geometry with Variable XS scheme which validate the precision of AP3-CRHOMO geometry with Variable XS scheme at core level calculation.

V. CONCLUSIONS

Accurate evaluation of control rod system characteristics is a one of the main issue of fast reactor evaluation regarding sustainable use of absorber materials. Current self-breeder core design need reduced reactivity margin for reactivity management and innovative control rod design involving alternative material such as hafnium or gadolinium may bring flexibility and improvement in this research field. To do so, advanced numerical methods implemented in APOLLO3® code system were tested and showed good accuracy towards Monte-Carlo reference calculations. The tabulated cross-section scheme improves significantly the accuracy on computation of reactivity variation. The benefit of MOC based calculation at lattice level combined with the ability to handle and treat unstructured geometries at core level bring new tools that enable to meet the designer requirements.

Although deeper study and improvement are required to cover the whole range of innovative configurations, the present calculation provides high level confidence to be used as reference tools for design purpose.

ACKNOWLEDGMENTS

APOLLO3® and TRIPOLI-4® are registered trademark of CEA. The first author would like to thank the APOLLO3® development team for their efforts in developing the code. We gratefully acknowledge AREVA and EDF for their long term partnership and their support.

REFERENCES

[1] C. Venard *et al.*, "The ASTRID core at the end of the conceptual design phase," *Proc FR*, vol. 17, 2017.

[2] J. Y. Moller, J. J. Lautard, and D. Schneider, "Minaret, a deterministic neutron transport solver for nuclear core calculations," presented at the M&C 2011, Rio de Janeiro, RJ, Brazil, 2011.

[3] D. Sciannandrone, S. Santandrea, and R. Sanchez, "Optimized tracking strategies for step MOC calculations in extruded 3D axial geometries," *Ann. Nucl. Energy*, vol. 87, pp. 49–60, Jan. 2016.

[4] Gérald Rimpault, Danièle Plisson, Robert Jacqmin, Jean Tommasi, and Robert Jacqmin, "THE ERANOS CODE AND DATA SYSTEM FOR FAST REACTOR NEUTRONIC ANALYSES," presented at the PHYSOR 2002, Seoul, Korea, 2002.

[5] E. Brun *et al.*, "TRIPOLI-4®, CEA, EDF and AREVA reference Monte Carlo code," *Ann. Nucl. Energy*, vol. 82, pp. 151–160, Aug. 2015.
[6] OECD Nuclear Energy Agency, I. David, and B. Francisco, *Benchmark for Neutronic Analysis of Sodium-cooled Fast Reactor Cores with Various Fuel Types and Core Sizes*. OECD Publishing, 2016.
[7] M. Coste-Delclaux, "Galilee: A nuclear data processing system for transport, depletion and shielding codes," presented at the WONDER 2009, Cadarache, FRANCE, 2009.
[8] P. Archier *et al.*, "New reference APOLLO3 calculation scheme for sodium cooled fast reactors: from sub-assembly to full-core calculations," presented at the PHYSOR 2016, Sun Valley, USA.
[9] P. Archier, S. M. Domanico, J.-M. Palau, and G. Truchet, "Validation of a Multi-Purpose Depletion Chain for Burnup Calculations through TRIPOLI-4 CALCULATIONS and IFP Perturbation Method," presented at the PHYSOR2016, Sun Valley, USA, 2016.
[10] J.-F. Vidal, "APOLLO3 Homogenization Techniques for Transport Core Calculation - Application to the ASTRID CFV Core," Jeju, Korea, 2017.
[11] V. Jouault, J. M. Palau, G. Rimpault, and J. F. Vidal, "A New Breakdown Methodology to Estimate Neutronic Model Biases Applied to APOLLO3® SFR Core Calculations," presented at the M&C 2017, Jeju, Korea, 2017.
[12] P. Archier, J.-M. Palau, and J.-F. Vidal, "Validation of the Newly Implemented 3D TDTMOC Solver of APOLLO3 Code on a Whole 3D SFR Heterogeneous Assembly," presented at the PHYSOR 2016, Idaho USA, 2016.
[13] Y.-K. Lee, E. Brun, and X. Alexandre, "SFR whole core burnup calculations with TRIPOLI-4 Monte Carlo code," presented at the PHYSOR 2014, Kyoto, JAPAN, 2014.
[14] A. Tsilanizara *et al.*, "DARWIN: An Evolution Code System for a Large Range of Applications," *J. Nucl. Sci. Technol.*, vol. 37, no. sup1, pp. 845–849, Mar. 2000.
[15] A.-M. Baudron and J.-J. Lautard, "MINOS: A Simplified Pn Solver for Core Calculation," *Nucl. Sci. Eng.*, vol. 155, no. 2, pp. 250–263, Feb. 2007.
[16] G. Rimpault *et al.*, "Objectives and Status of the OECD/NEA sub-group on Uncertainty Analysis in Modelling (UAM) for Design, Operation and Safety Analysis of SFRs (SFR-UAM)," presented at the FR17, Yekaterinburg, Russian Federation, 2017, vol. 17.
[17] G. Rimpault, "Algorithmic Features of the Ecco Cell Code for Treating Heterogeneous Fast Reactor Subassemblies," presented at the Proc. Int. Top. Meet. on Reactor Physics and Computations, Portland, Oregon, 1995.
[18] C. B. Carrico, E. E. Lewis, and G. Palmiotti, "Three-Dimensional Variational Nodal Transport Methods for Cartesian, Triangular, and Hexagonal Criticality Calculations," *Nucl. Sci. Eng.*, vol. 111, no. 2, pp. 168–179, Jun. 1992.
[19] J.-F. Vidal *et al.*, "APOLLO3 ® Homogenization Techniques for Transport Core Calculations - Application to the ASTRID CFV Core," *Nucl. Eng. Technol.*, Sep. 2017.
[20] D. Blanchet and B. Fontaine, "Control Rod Depletion in Sodium-Cooled Fast Reactor: Models and Impact on Reactivity Control," *Nucl. Sci. Eng.*, vol. 177, no. 3, pp. 260–274, Jul. 2014.
[21] M. Andersson, "Control rod homogenization in heterogeneous sodium-cooled fast reactors," Doctor, Chalmers University of Technology, Göteborg, Sweden, 2016.